**Biogeosciences
Discussions**

Biogeosciences Discussions is the access reviewed discussion forum of *Biogeosciences*

Measurement depth effects on the apparent temperature sensitivity of soil respiration in field studies

A. Graf, L. Weihermüller, J. A. Huisman, M. Herbst, J. Bauer, and H. Vereecken

Forschungszentrum Jülich, Agrosphere Institute (ICG-4), Institute for Chemistry and Dynamics of the Geosphere, 52425 Jülich, Germany

Correspondence to: A. Graf (a.graf@fz-juelich.de)

BGD

5, 1867–1898, 2008

Temperature measurement depth effects

A. Graf et al.

Title Page

Abstract	Introduction
Conclusions	References
Tables	Figures

Back | Close

Full Screen / Esc

Printer-friendly Version

Interactive Discussion

Temperature measurement depth effects

A. Graf et al.

Abstract

CO_2 efflux at the soil surface is the result of respiration in different depths that are subjected to variable temperatures at the same time. Therefore, the temperature measurement depth affects the apparent temperature sensitivity of field-measured soil respiration. We summarize existing literature evidence on the importance of this effect, and describe a simple model to understand and estimate the magnitude of this potential error source for heterotrophic respiration. The model is tested against field measurements. We discuss the influence of climate (annual and daily temperature amplitude), soil properties (vertical distribution of CO_2 sources, thermal and gas diffusivity), and measurement schedule (frequency, study duration, and time averaging). Q_{10} as a commonly used parameter describing the temperature sensitivity of soil respiration is taken as an example and computed for different combinations of the above conditions. We define conditions and data acquisition and analysis strategies that lead to lower errors in field-based Q_{10} determination. It was found that commonly used temperature measurement depths are likely to result in an underestimation of temperature sensitivity in field experiments. Our results also apply to activation energy as an alternative temperature sensitivity parameter.

1 Introduction

Soil respiration is increasingly recognized as a major factor in the global carbon cycle. Due to a rising interest in the feedback between soils and climate change, numerous studies have provided relations between temperature and soil respiration either obtained in the laboratory or in the field. Typically, the temperature sensitivity of soil respiration is expressed as the Q_{10} value, i.e. the factor by which respiration is enhanced at a temperature rise of 10 K (Appendix A).

Several restrictions to the significance of the Q_{10} concept, especially if mistaken as a means to extrapolate soil CO_2 losses into a warmer future, have been brought up

(Davidson and Janssens, 2006). Here, we examine an additional restriction which has received remarkably little attention in literature. In most field studies, column-integrated soil respiration and its sensitivity are quantified by a single temperature measurement, while the total flux is a sum of source terms from various depths, which are exposed
⁵ to different temperature regimes. Because of the attenuation and phase shift of temperature fluctuations with increasing depth, the apparent Q_{10} will depend on the temperature measurement depth. This possibility was mentioned first by Lloyd and Taylor (1994), but without quantification. Davidson et al. (1998) predicted that Q_{10} values would increase with temperature measurement depth, and recognized that this com-
¹⁰ plicates comparisons between studies. Recently, several field studies with multiple temperature measurement depths have been published (Xu and Qi, 2001; Hirano et al., 2003; Tang et al., 2003; Gaumont-Guay et al., 2006; Khomik et al., 2006; Shi et al., 2006; Wang et al., 2006). All of them show an increase of apparent Q_{10} with depth. The same effect has also been identified in model simulations by Hashimoto et al. (2006).
¹⁵ To our knowledge, no explanations of the varying shape of these relationships have been provided so far. In addition, it is unclear which Q_{10} value, if any, is most appropriate when temperature measurements at multiple depths are available. Tang et al. (2003), Perrin et al. (2004) and Shi et al. (2006) use the temperature measurement depth yielding the highest R^2. Gaumont-Guay et al. (2006) suggest that the tempera-
²⁰ ture - efflux curve with the lowest hysteresis indicates the most appropriate temperature measurement depth. Since most studies use a single, more or less arbitrary, temperature measurement depth, the effect of varying temperature measurement depth is often not considered.

The aim of this study is to quantify the error in Q_{10} determination caused by different
²⁵ temperature measurement depths as a function of soil properties, climate, and measurement schedule. To this end, we present a simple model and validate it against field measurements of heterotrophic respiration. We consider this model as a tool that helps with the design of field studies with meaningful temperature measurement depths, and with a more appropriate interpretation of existing datasets.

A. Graf et al.

2 Methods

2.1 Literature review

We found eight studies where multiple temperature measurement depths were used to derive apparent Q_{10} depth profiles. An overview about the flux methods, site charac-
5 teristics, and time schedules is given in Table 1.

Two of these studies use continuous CO_2 concentration profile measurements in the soil to calculate half-hourly surface CO_2 effluxes validated against chamber measure-ments. All other studies directly use a closed chamber system to measure CO_2 efflux. The temporal resolution of the studies differ. Many studies use a nested approach with
10 one or more measurement days each month, and two to ten measurements per such day. Some studies cover a period of less than a year, whilst others leave out the winter months for operational reasons. Land use of the sites includes forests, savannah, and farmland, and the climate is ranging from subtropical to boreal.

We also obtained Q_{10} values from studies with a single, reported temperature mea-
15 surement depth (Kim and Verma, 1992; Dugas, 1993; Davidson et al., 1998; Fang et al., 1998; Chen et al., 2002; Law et al., 2002; Borken et al., 2003; Lou et al., 2003; Sav-age and Davidson, 2003; Yuste et al., 2003; Novick et al., 2004; Takahashi et al., 2004; deForest et al., 2006; Humphreys et al., 2006; Moyano et al., 2008; Tang et al., 2008). Here, either chamber or micrometeorological systems were used to measure soil CO_2
20 efflux. In some studies, air temperature was used to calculate the Q_{10}. It should be noted that most studies addressed total soil respiration, without differentiation between heterotrophic and autotrophic respiration.

2.2 Model

The model is based on the concept of thermal diffusion and is implemented in For-
25 tran95. An overview of the model architecture is given in Fig. 1 and the theory behind the model is described in the Appendix. In brief, a simplified infinite near-surface tem-

perature time series is generated using several distinct sine waves. The annual and diurnal cycle have a phase shift to correctly reproduce times of maxima and minima, assuming that $t=0$ is new year's midnight. A further cycle with a period of 12 h, a phase shift of 1 h, and an amplitude $A=A_{diurnal}/4$ was used to mimic the skewness of the daily temperature cycle due to slow cooling during the night. Variations of the diurnal amplitude and day length were not considered. The average temperature was set to the global average (15°C) in the numerical experiments, and equalled the average measured temperature (12.7°C) in the model validation. Input amplitudes are determined for the uppermost temperature sensor (0.5 cm) in the model validation. In the numerical experiments, amplitudes were provided for a reference depth of 5 cm. The reason is that amplitudes in this depth are more similar to air temperature than the soil surface temperature. Air temperature amplitudes are globally available and provide a more common reference than surface temperature.

The generated near-surface temperature time series is transferred to other soil depths using an analytical solution of the thermal diffusion equation. This solution does not consider time-variant thermal diffusivity. Instead, we use an effective thermal diffusivity representing the time averaged effect of soil moisture at each depth. On the other hand, time average effective thermal diffusivity may vary strongly with depth due to differences in soil properties and water content. To account for this, the analytic solution was applied in discrete depth steps of 1 cm, using the amplitudes and phase shifts in each layer to calculate those of the next deeper layer (Fig. 1). The model is run with a time step of 1 h. Soil respiration is calculated from temperature using the Q_{10} concept and, as an alternative, also using the Arrhenius concept (see Appendix A). The source strength of respiration at the average temperature is also given as a depth-dependent value. Here, only a relative vertical distribution is required because absolute values have no effect on the resulting apparent Q_{10} profile.

If CO_2 diffusion time from each depth to the soil surface is assumed to be insignificant, the efflux can simply be calculated by integration of the respiration over all depths. However, in analogy to the impact of thermal diffusion on the apparent Q_{10} discussed

above, slow gas diffusion could also affect the apparent Q_{10}. To test this hypothesis, we also included CO_2 diffusion in several model runs. As already proposed for heat diffusion, we use an effective diffusivity $D_{CO_2}\theta_a^{-1}$ (Appendix) invariant in time but vertically distributed. Because the concentration profiles are a result of the vertical source distribution and the nonlinear temperature dependence, CO_2 diffusion cannot be solved analytically. Therefore, we implemented a numerical solution (Appendix). The CO_2 flux between two adjacent layers is now the product of diffusivity and the concentration gradient. We assume no vertical exchange between the lowest layer and the underground. At the surface, a constant atmospheric CO_2 concentration of $16.5\times10^3\ \mu\text{mol m}^{-3}$ is maintained. The model considering diffusion requires initialization of the concentration profile. Therefore, the model uses a spin-up period. The length of the spin-up period is considered adequate when the difference in cumulative efflux between runs with and without diffusion is less than 1%.

Finally, the modelled time series of efflux at the surface and temperature in each depth are used to simulate the current practice of field-based Q_{10} determination. For each depth, regression of log-transformed efflux against temperature T is used to compute Q_{10}. To also test fitting of the Arrhenius relation, the inverse of the temperature is plotted against the respiration. In this case, the resulting activation energy is converted into a Q_{10} at the study's average temperature for comparison (cf. Sanderman et al., 2003).

2.3 Field measurements

An automated soil CO_2 flux chamber system (Li-8100, Li-Cor Inc., Lincoln, Nebraska, USA) was operated with four type T thermocouple thermometers at the FLOWatch project test site Selhausen of the Forschungszentrum Jülich. The test site is located in the river Rur catchment (50°52′09″ N, 06°27′01″ E, 104.5 m above sea level). The soil is an Orthic Luvisol and the texture is silt loam according to the USDA classification. A detailed description of the test site is given by Weihermüller et al. (2007b).

Temperature measurement depth effects

A. Graf et al.

Organic carbon content was determined in vertical steps of 15 cm. In September 2006, the soil was tilled up to a depth of 15 cm and power harrowed. Bare field conditions were maintained by a repetition of this treatment in April 2007, several applications of glyphosate, and manual weed control at the efflux measurement plot. Historically, the field was annually ploughed to a depth of 30 cm, and the crop rotation was sugar beet –winter wheat. From 15 October 2006 to 24 April 2007 only one CO_2 flux system was used (closing interval every 30 min). From 24 April to 14 October 2007, four identical chambers with a separation of 20 cm were operated with the Li8100 multiplexer system (closing interval 15 min for each chamber). The soil flux chambers were placed on soil collars of 20 cm in diameter and a height of 7 cm, which were inserted 5 cm into the soil. The system was closed for two minutes for each flux measurement. CO_2 and water vapour concentration as well as chamber headspace temperature were measured every second, and the CO_2 concentration was corrected for changes in air density and water vapour dilution. The soil respiration was calculated by fitting a linear regression to the corrected CO_2 concentrations from 30 s after closing until reopening.

The thermocouples used to measure soil temperature have 1 mm thick unshielded joints to ensure a quick response, and were installed horizontally at 0.5, 3, 5, and 10 cm depth, 20 cm away from the chamber system. Temperature data were logged every second while the chamber was closed, and averaged. To vertically extend the empirical apparent Q_{10} profiles, we also use temperature data of pF-meters (Ecotech, Bonn, Germany) in 15, 30, 45, 60, 90 and 120 cm depth, which were logged independently in 1 h intervals.

To obtain a uniform dataset, the efflux and temperature measurements were reduced to median hourly CO_2 flux and average hourly soil temperature at each measurement depth. In the case of CO_2 flux, the median was used because it is less sensitive to outliers and non-normal distributions. In the final data set, only those hours were considered where all flux and temperature measurements were available. Because more than 50% of the hours in December and January could not be considered due to power supply problems, these two months were completely excluded from the dataset.

Temperature measurement depth effects

A. Graf et al.

Title Page

Abstract | Introduction

Conclusions | References

Tables | Figures

|◄ | ►|

◄ | ►

Back | Close

Full Screen / Esc

Printer-friendly Version

Interactive Discussion

To determine the effective soil thermal diffusivity, we derived the annual amplitude in each depth from average daily temperature, and applied the phase equation (e.g., Verhoef et al., 1996) to each pair of successive temperature measurement depths. Linear regression provided D_T values for each depth increment.

3 Results

3.1 Literature and own field measurements

Figure 2 shows apparent Q_{10} values as a function of depth from this and other studies. An increase of apparent Q_{10} with depth can be seen in all studies, but with a strongly variable slope. The highest apparent value (Gaumont-Guay et al., 2006, Q_{10}=150 in a temperature measurement depth of 50 cm) is not shown for scaling reasons. This profile is based on measurements taken during two winter months. The second highest value was found by Khomik et al. (2006), also at 50 cm, in long-term measurements excluding winter months, but including snow cover situations in spring, and capturing the diurnal cycle in summer (Table 1). Of the remaining profiles, our own measurements and those by Shi et al. (2006), both from farmland and capturing the diurnal cycle, increase strongest with depth. The remaining profiles exhibit comparatively low, but still substantial apparent Q_{10} increases with depth. In the study by Perrin et al. (2004), the air temperature 9 m above ground level is included and yields a considerably lower value than the three soil temperature series, which are close to each other both in measurement depth and in apparent Q_{10}.

The values from studies using a single temperature measurement depth also show Q_{10} values increasing with depth.

3.2 Model validation

Figure 2 also shows the best model fit (RMSE of 0.16) obtained by fitting a depth invariant input Q_{10}, while assuming a model domain of 50 cm, a homogeneous carbon

Temperature measurement depth effects

A. Graf et al.

source distribution within the plough layer (0 to 30 cm depth) and a carbon-free subsoil and neglecting CO_2 diffusion. The depth-invariant input Q_{10} yielding this optimum fit was 5.9. We did not consider depth-dependent values of the input Q_{10} in order to avoid over-fitting. It should be noted that the results were not substantially different when using an Arrhenius relationship instead of the Q_{10} concept (not shown). This also applies to all results shown below.

The model fit was less good when using the measured, linearly interpolated C_{org} profile (Fig. 3) as a proxy of the source strength distribution. Increasing the length of the model domain to 120 cm also decreased model quality (Table 2). The optimal input Q_{10} values found for these different conditions vary from 5.3 to 6.2, and would have been directly measured in depths between 10 cm and 20 cm. Considering CO_2 diffusion either led to negligible differences or higher errors, depending on diffusivity (also see next sections).

3.3 Numerical experiments

The validated model was used to study the effect of several factors on the apparent Q_{10} profile. Figure 4 shows apparent Q_{10} values as a function of both temperature measurement depth and each factor considered in this study. The depth where the R^2 between soil respiration and temperature is highest is indicated with R^2_{max}. The input Q_{10} used to generate all plots is 2.5.

In the case of a homogenous respiring A-horizon of varying thickness above a non-respiring subsoil (Fig. 4a), the input Q_{10} is obtained at about half the depth of the respiring layer. The highest R^2, however, is found at a shallower depth. The difference between the optimal measurement depth and the depth with the highest correlation increases with the thickness of the respiring layer (up to 10 cm for a 50 cm thick respiring layer). The apparent Q_{10} at the depth of highest R^2, however, does not differ more than 5% from the input value. Typical measurement depths used in field studies (0 to 10 cm) result in errors ranging from −30 to +10 % depending on the depth of the respiring

layer. The apparent Q_{10} values shown in Fig. 4a vary from less than 1.8 to more than 3, which is about the range of most reported values (Raich and Schlesinger, 1992), although the input Q_{10} was constant at 2.5. In all other plots (Fig. 4b to f), we assumed a respiring layer thickness of 30 cm.

The impact of the length of the measurement period is illustrated in Fig. 4b. For short periods (less than about 180 days), the apparent Q_{10} behaves highly irregular. For measurement periods longer than a year, the apparent Q_{10} is stable throughout the first 20 cm depth. It should be noted that we assumed that inter-annual variations in average temperature can be neglected here. All other plots are based on a 1 year measurement period.

Changing the thermal diffusivity of the soil (one value for all depths, Fig. 4c), yields an irregular behaviour for values less than $0.1\,\mathrm{mm^2\,s^{-1}}$. Above this threshold, possible apparent Q_{10} errors, as well as the distance between the Q_{10} obtained from the highest R^2 and the input Q_{10}, decreases with increasing diffusivity. We used a thermal diffusivity of $0.5\,\mathrm{mm^2\,s^{-1}}$ in all other plots.

The influence of CO_2 transport is neglected in all simulations except for those presented in Fig. 4d. Considering gas diffusion leads to an offset in apparent Q_{10} in the first 20 cm compared to cases where diffusion is not considered, but the extent of this offset is less than 2% for effective diffusivities greater than $0.5\,\mathrm{mm^2\,s^{-1}}$. Below $0.5\,\mathrm{mm^2\,s^{-1}}$, this offset increases sharply and the depth of the highest R^2 can be found below rather than above the depth regaining the input Q_{10}.

In Fig. 4e, the annual temperature amplitude was varied from 0 to 20 K (twice the value used in the other model runs). For annual amplitudes below the diurnal amplitude of 5 K, the resulting profile is highly irregular with a local maximum. In addition, the temperature sensitivity is underestimated throughout most of the modelling domain. Figure 4f shows the effect of varying diurnal amplitudes. High diurnal amplitudes increase the errors made within the first 20 cm, and lead to an underestimation of temperature sensitivity when using shallow temperature sensors. Zero diurnal temperature amplitudes yield an almost linear apparent Q_{10} profile and a close proximity

Full Screen / Esc

Printer-friendly Version

Interactive Discussion

of the depth with the highest R^2 and the input Q_{10}. Note that in our numerical experiments, this behaviour could be reproduced using daily averages of temperature and CO_2 efflux. Averaging efflux before or after log-transformation only resulted in negligible differences ($\Delta Q_{10} < 0.01$). Simulating only one measurement per day at a fixed time
5 also yields similar results, but with a small vertical offset of about 3 cm depending on the time of day of the measurement.

4 Discussion

4.1 Literature and own field measurements

The variability of the Q_{10} dependence on temperature measurement depth underlines
10 the need for a methodology that allows comparison of temperature sensitivities determined in field experiments. Various explanations for the variability of apparent Q_{10} profiles can be deduced from our modelling exercise. The highest reported apparent Q_{10} (Gaumont-Guay et al., 2006) is based on those authors' deepest temperature measurements and a short study period of two months. The amplitude of the diurnal
15 temperature is strongly attenuated at that depth, and the amplitude of the annual cycle is not fully sampled because of the short measurement period. Therefore, CO_2 efflux was correlated to temperature values with small amplitude and high phase shift, which can result in very high or very low apparent Q_{10} values. The second highest Q_{10} increase with depth (Khomik et al., 2006) originates from a study capturing the daily
20 temperature cycle in summer, with additional less frequent measurements in spring and autumn, and no measurements in winter. The steep profiles found by Shi et al. (2006) and by ourselves were obtained for agricultural soils without temperature attenuation effects on the diurnal cycle by abundant vegetation. The lowest increase of Q_{10} with depth was found in a study where measurements of the diurnal cycle of CO_2 efflux
25 were avoided (Wang et al., 2006). The air temperature in proximity to the forest canopy included by Perrin et al. (2004) is supposed to have a higher diurnal amplitude than

forest soil temperatures and consequently yields a lower apparent Q_{10}.

Vegetation does not only affect the temperature regime of the soil, but also respiration itself. All studies discussed here except for our own bare soil measurements include both heterotrophic and root respiration. Hanson et al. (2000) review various studies on the contribution of root to total soil respiration. Depending on ecosystem, they find that 10 to 90% of total respiration stems from roots with an average contribution of about 50%. Root respiration is related not only to those environmental variables that are known to influence heterotrophic respiration, but also to aboveground plant productivity and thus to radiation (Tang et al., 2005). This correlation is subject to a lag between several hours and several days (Moyano et al., 2008), due to the time taken by phloem transport from leaves to roots. The similarity between this lagged response to radiation and soil temperature at a certain depth, which may also be considered a lagged response to radiation, could cause confusion. In the interpretation of mixed soil respiration, too much of temporal variability might be attributed to either soil temperature or aboveground radiation, depending on normalisation procedure and the available temperature measurement depth. In general, however, we may expect the presence of another controlling factor to weaken the depth dependence of the apparent Q_{10}. This would be in good agreement with the fact that dense and high forest sites generally seem to yield somewhat more stable profiles in Fig. 2, as would the damping effect of the canopy on the temperature regime.

4.2 Model validation

The model application to the field data demonstrates that the model is able to describe the temperature sensitivity variation with depth. The remaining uncertainty of about ±10% occurs when considering deeper layers, and their carbon content (Table 2). We attribute this to two main causes. First, temperature measurement errors become increasingly significant deeper in the soil, where amplitudes are smaller. Such errors are not simulated by the model. However, temperature sensitivity of soil respiration is rarely determined from temperature sensors installed in large depths. Second, there is

Temperature measurement depth effects

A. Graf et al.

|◄ | ►|

◄ | ►

Back | Close

Full Screen / Esc

Printer-friendly Version

Interactive Discussion

considerable uncertainty in the source strength distribution. Organic carbon content includes accumulated stable carbon pools, the fraction of which can be depth-dependent itself. The field data were best described when neglecting the organic carbon content found below the A-horizon. This seems to indicate that deeper carbon is less involved

5 in respiration activity, which is in good agreement with the general assumption that carbon pools in deeper horizons are more stable (cf. Fierer et al., 2003). The increasing uncertainty with depth also implies that field measurements of CO_2 efflux at the soil surface are not suited to derive the temperature sensitivity of deep buried carbon, which has been associated with higher temperature sensitivities by some (Knorr et al.,

10 2005; Davidson and Janssens, 2006). Our study shows that although a true increase of Q_{10} with depth may be present, it should not be confused with the temperature measurement depth dependence of the apparent Q_{10}.

It was not necessary to consider CO_2 diffusion to model the apparent Q_{10} variation with depth for our field experiment. This fits well with the results of the numerical

15 experiments discussed in the next section, which showed that for most diffusivities observed in the field the impact should be low (Fig. 4d; Tang et al., 2003; Werner et al., 2004). Nevertheless, a general recommendation to neglect CO_2 transport should not be made based on the results of a single field study.

It is noteworthy that the measurement depths that would have yielded a Q_{10} value

20 in the range of the optimal input Q_{10} of the model, are below 10 cm, while all single measurement depths found in our literature study are above that depth. At least in the case of this site, relying on literature conventions would thus have likely underestimated temperature sensitivity.

Finally, it should be mentioned that the model only considers the pure confounding

25 factor temperature measurement depth. Depending on the site characteristics, other confounding effects, such as correlation of temperature with moisture (Davidson et al., 1998), may cause errors of similar magnitude in field-based Q_{10} determination. In the frequent case of negative correlation between temperature and moisture, the result will again be an underestimation of temperature sensitivity.

4.3 Numerical experiments

When the vertical source strength distribution consists of a homogenous respiring layer above a non-respiring sub-soil, the best depth to place a single temperature sensor is the centre of the respiring layer (Fig. 4a). Although such a distribution is not unrealistic for our field reference dataset, it may be not fulfilled in non-agricultural soils, especially in the presence of litter layers. As an alternative method to determine the most appropriate depth, Tang et al. (2003), Perrin et al. (2004) and Shi et al. (2006) suggested the maximum R^2 criterion. Although our numerical experiments show that this is not exactly correct, it is a good approximation in most conditions. However, both the R^2 criterion and the centre placement fail in extreme conditions, as illustrated in Fig. 4b to e.

The difference between the depth of highest R^2 and the depth regaining the input Q_{10} is a result of the combined effect of amplitude attenuation and phase shift of temperature waves. For an infinitely thin respiring layer, the R^2 is highest for a temperature measurement within this layer. This measurement will also provide the correct Q_{10}. At other depths, the R^2 is lower due to phase shifts in the temperature time series. For thicker respiring layers, efflux at the surface integrates over CO_2 production time series with different delays and amplitudes. If the delay is considered in isolation, the highest R^2 would occur in the middle the respiring layer. However, the apparent Q_{10} would underestimate the temperature sensitivity for all depths because the averaging of several phase-shifted temperature waves results in a smaller range of temperature values. When amplitude attenuation and phase shifts are both considered, deeper parts of the respiring layer show a smaller variance in both, temperature and their contribution to column respiration. Therefore, the depth of highest R^2 is shifted upwards. At the same time, the lower temperature amplitudes in these depths counteract the underestimation of the apparent Q_{10}. Strictly spoken, the temperature measurement depth regaining the input Q_{10} is not a "correct" depth, but a depth where positive and negative errors are balanced.

Temperature measurement depth effects

A. Graf et al.

The depth that regains the input Q_{10} will not always be within the respiring layer, as illustrated by Fig. 4b. In this figure, the length of the measurement period was varied. The model qualitatively confirms that extremely high apparent temperature sensitivities for greater measurement depths, such as those found by Gaumont-Guay et al. (2006) and Khomik et al. (2006), can be caused by incomplete representation of the annual cycle. For a more quantitative assessment, too little is known especially on the varying thickness and thermal properties of the snow cover, which was an important feature in both studies. The fact that measurement periods of less than half a year can result in high Q_{10} errors is also relevant to studies separating the study period into seasons to capture plant phenological effects on temperature sensitivity (e.g., Xu and Qi, 2001; Yuste et al., 2004; deForest et al., 2006).

Variation of the soil thermal diffusivity (Fig. 4c) confirms the expectation that accurate field-based Q_{10} measurements are more likely when temperature waves propagate rapidly into the ground. According to Zmarsly et al. (2002), most soils have thermal diffusivities ranging between 0.1 (dry organic) and $0.75\,\text{mm}^2\,\text{s}^{-1}$ (wet sand). Therefore, the irregular behaviour of the apparent Q_{10} for very low diffusivities is not relevant in most ecosystems.

Effective CO_2 diffusivities can cover a much larger range. A compilation of Werner et al. (2004) based on 81 studies shows that $D_{CO_2}\theta_a^{-1}$ can range from 0.09 to more than $12\,\text{mm}^2\,\text{s}^{-1}$. Despite this large range, our numerical experiment shows that the influence of diffusion on apparent Q_{10} would be negligible for all but the three lowest values summarized by Werner et al. (2004). It is interesting that for such small diffusivities, the depth of highest R^2 can drop below the depth regaining the input Q_{10}. We attribute this to the fact that the time series of surface efflux is now delayed compared to the temperature time series in those depths where most of the CO_2 is produced. Consequently, efflux correlates better with deeper temperature time series. This is no indication of a causal relationship, as the CO_2 produced in these depths is delayed even stronger before reaching the surface.

An evaluation of the effect of annual temperature amplitude (Fig. 4e) is relevant to

avoid systematic errors when temperature sensitivities from different climatic zones are compared. Close to the equator where the annual amplitude is low, field-based determination of accurate Q_{10} values is difficult. Typically, the temperature sensitivity will be underestimated. Continental and boreal climates with high annual amplitudes

5   potentially allow an accurate determination of the Q_{10} when the measurement period is long and continuous. This may be difficult in case of harsh winter conditions, or be complicated by the thermal properties of a snow cover (see above).

The numerical experiment on diurnal amplitude (Fig. 4f) is of particular interest because the positive effects of low diurnal amplitudes can be approximated by daily av-

10 eraging of efflux and temperature time series. A similar reduction in daily amplitude can be obtained by measurements at a fixed time of day, but it remains to be examined whether this alternative is more susceptible to varying day lengths and amplitudes throughout the year.

5   Conclusions

15 We described the development, validation, and application of a simple model to explain and estimate the errors in temperature sensitivity determination related to the temperature measurement depth. We chose the widely used Q_{10} concept as an example, but the alternative activation energy concept provides almost identical results.

Depending on study conditions, the vertical profile of the apparent Q_{10} may range

20 from fairly regular to highly irregular. The latter case can include local minima and maxima, decoupling of the depth of correct Q_{10} from the depth of highest R^2, and cases where the obtained Q_{10} is incorrect for all conventional temperature measurement depths. In these cases, only laboratory incubation experiments directly can yield correct temperature sensitivity relations, although these experiments are not free of

25 errors and assumptions either. An alternative possibility would be to inversely estimate the Q_{10} using numerical models of CO_2 production, CO_2 transport and heat transport applied to field data. This approach has recently been used to estimate soil physical

Temperature measurement depth effects

A. Graf et al.

properties and CO_2 source strength (Herbst et al., 2008; Novak, 2007; Weihermüller et al., 2007a) and could be extended to Q_{10} estimation.

In many field studies, however, the detailed input data required to drive mechanistic CO_2 models are not available. In such cases, the model presented here, and some basic climate and soil data, may help reducing errors in temperature sensitivity analysis. However, validation has shown that an uncertainty remains due to the choice of input parameters. Also, analyses of additional field data sets to test whether the simplifications made within the model are justified would be desirable. Nevertheless, the model clearly helps recognizing field study conditions where Q_{10} determination is fairly reliable. The following conditions allow an accurate estimation of Q_{10}:

- a thin and easily distinguished horizon of respiration activity,

- a measurement period of one year or more,

- a high thermal and CO_2 diffusivity of the soil,

- a high annual temperature amplitude,

- daily averaging of measurements before fitting the temperature sensitivity function.

Our analyses indicate that a temperature measurement depth within the upper 10 cm, as is commonly used in field studies, is likely to result in an underestimation of temperature sensitivity, at least in the absence of a litter layer. According to the latest IPCC report (Solomon et al., 2007), most models used to estimate the biochemical feedback of land surfaces to climate change assume a soil respiration Q_{10} close to 2. It is noteworthy that this assumption is based on averaging not only laboratory but also field studies (Solomon et al., 2007), e.g. those compiled by Raich and Schlesinger (1992). These models predict a global effective sensitivity of heterotrophic respiration of 6.2% per K warming. However, a larger Q_{10} of 2.5 would be well within the uncertainty range identified in this study. This would increase global sensitivity by about one

third in each model, which is the same order of magnitude as the standard deviation among the models. The models give an average absolute sensitivity of land surfaces to climate change of -79 Gt sequestered carbon per K warming, although this rate is highly variable between the models (± 45 GtC K^{-1}). An additional uncertainty of one third due to an unknown primary temperature sensitivity of respiration, divided by the time span over which such a 1 K increase is assumed to occur (40 to 50 years depending on scenario), would be equal to 7 to 9% of the current annual emissions from fossil fuel burning and cement production.

Appendix A

Temperature sensitivity functions

Two methods are most commonly used to relate temperature and respiration. The first is an empirical exponential relationship suggested by van t'Hoff (e.g., Yuste et al., 2004):

$$SR = SR_{T_{\text{ref}}} e^{\frac{\ln Q_{10}}{10}(T - T_{\text{ref}})} \tag{A1}$$

where SR is soil respiration (µmol m^{-2} s^{-1}), T is temperature (K) and T_{ref} is an arbitrary reference temperature with a know respiration rate $SR_{T_{\text{ref}}}$. Q_{10} is the rate by which respiration changes with a temperature change of 10 K. The Q_{10} is a commonly used parameter to report the temperature sensitivity of soil respiration. The second relationship is more physically based and uses activation energy considerations introduced by Arrhenius (e.g., Lloyd and Taylor, 1994):

$$SR = SR_{T_{\text{ref}}} e^{\frac{E_a}{RTT_{ref}}(T - T_{\text{ref}})} \tag{A2}$$

Here, E_a is the activation energy (J mol^{-1}), and $R=8.314$ J mol^{-1} K^{-1} is the universal gas constant. Further temperature sensitivity functions are summarised by Kätterer et

Temperature measurement depth effects

A. Graf et al.

Title Page

Abstract | Introduction

Conclusions | References

Tables | Figures

◀ | ▶

◀ | ▶

Back | Close

Full Screen / Esc

Printer-friendly Version

Interactive Discussion

al. ([1998](#)) and Bauer et al. ([2008](#)). The temperature sensitivity coefficients of these methods (Q_{10} and E_a) are not equivalent. For typical temperature and respiration ranges, a Q_{10} value derived from Eq. (A2) based on E_a decreases slowly with increasing temperature, whereas Q_{10} is a constant in Eq. (A1). A slow Q_{10} decrease with
5   increasing temperature has been reported in a range of field and laboratory studies (e.g., Kirschbaum, 2006; Shi et al., 2006). Large differences between both relations only occur in the case of extrapolation, especially into warmer conditions. However, it has been questioned whether extrapolation can be used for future feedback prediction (Davidson and Janssens, 2006). One reason for this is that different soil carbon pools
10   may have different temperature sensitivities. A long-term temperature change would then change the pool ratios and, consequently, the effective temperature sensitivity of the soil. It is still under debate whether these effects are of a measurable and relevant magnitude or not (Fang et al., 2005; Knorr et al., 2005; Reichstein et al., 2005; Conen et al., 2006; Larinova et al., 2007).

15 **Appendix B**

Theory of soil temperature profiles

Soil surface temperature changes are mainly induced by the radiation balance at the soil surface and exchange of sensible and latent heat between the soil and the atmo-
20   sphere. The variation in soil surface temperature propagates into deeper layers. In the absence of transport of sensible and latent heat in the soil gas phase (Weber et al., 2007), this process is controlled by the soil thermal diffusivity D_T ($\mathrm{m^2\,s^{-1}}$):

$$\frac{\partial T}{\partial t} = D_T \frac{\partial^2 T}{\partial z^2} = \frac{\lambda}{\rho c} \frac{\partial^2 T}{\partial z^2} \tag{B1}$$

where t is time (s) and z is depth (m). Thermal diffusivity is a function of thermal
25   conductivity λ ($\mathrm{W\,m^{-1}\,K^{-1}}$), heat capacity c ($\mathrm{J\,kg^{-1}\,K-1}$), and bulk density ρ ($\mathrm{kg\,m^{-3}}$).

1885

The typical order of magnitude of soil thermal diffusivity is 10^{-7} to $10^{-6}\,\mathrm{m^2\,s^{-1}}$ (Zmarsly et al., 2002). To transfer a soil temperature time series to another depth, it is often represented by a series of sine waves (de Vries, 1963; Verhoef et al., 1996; Heusinkveld et al., 2004; Graf et al., 2008):

$$T = \overline{T} + \sum_{i=1}^{n} A_i \sin \frac{2\pi(t + \Delta t_i)}{\tau_i} \tag{B2}$$

where $\overline{T}$ denotes the average temperature (K), A_i is the temperature amplitude (K), τ_i is the period length (s), and Δt_i the phase shift (here in units of time and therefore included in the bracketed term) of the sine wave indexed i. When thermal diffusivity is constant with depth and time, there is an analytical solution to Eqs. (B1) and (B2) (de Vries, 1963) that predicts temperature in any other depth (Heusinkveld et al., 2004; Graf et al., 2008):

$$T = \overline{T} + \sum_{i=1}^{n} A_i \exp\left(\Delta z \sqrt{\frac{\pi}{D_T \tau_i}}\right) \sin \frac{2\pi(t + \Delta t_i + \frac{\Delta z \tau_i}{2\pi}\sqrt{\frac{\pi}{D_T \tau_i}})}{\tau_i} \tag{B3}$$

where Δz is the difference between the actual and the reference depth. Stepwise application of Eq. (B3) allows to treat thermal diffusivities that change along a vertical profile (cf. methods section).

Appendix C

Theory of gas diffusion

Diffusion of CO_2 through soil air is described by:

$$\frac{\partial c}{\partial t} = \tau \theta_a D_a \frac{\partial^2 c_a}{\partial z^2} + SR \tag{C1}$$

where c is the total volumetric concentration of CO_2, c_a is the concentration in soil air, D_a is the diffusivity of CO_2 in air ($\text{m}^2\,\text{s}^{-1}$), θ_a (dimensionless) is the soil air content, and τ is a dimensionless tortuosity factor. D_a, the soil air content, tortuosity and other factors such as transport through soil water and pressure turbulence can be combined into an effective diffusivity (Simunek and Suarez, 1993; Hirano et al., 2003; Tang et al., 2003; Takle et al., 2004). In this study, we use a wide range of field-determined effective diffusivities reviewed by Werner et al. (2004). To solve Eq. (C1), we use an explicit time discretization:

$$c(t + \Delta t, z) = c(t, z) + \Delta t (SR(t, z) + D_{CO_2}(z - \tfrac{1}{2}\Delta z)\frac{c(t, z - \Delta z) - c(t, z)}{\theta_a \Delta z^2}$$

$$- D_{CO_2}(z + \tfrac{1}{2}\Delta z)\frac{c(t, z) - c(t, z + \Delta z)}{\theta_a \Delta z^2}) \tag{C2}$$

By defining D_{CO_2} in planes 0.5 Δz above and below all other depth-dependent input data, we achieve mass-consistency. The maximum value of the time-step for a stable solution is $\Delta t < 0.5 \Delta z^2 D_{CO_2}^{-1} \theta_a$.

Title Page

Abstract | Introduction

Conclusions | References

Tables | Figures

◀ | ▶

◀ | ▶

Back | Close

Full Screen / Esc

Printer-friendly Version

Interactive Discussion

References

Bauer, J., Herbst, M., Huisman, J. A., Weihermüller, L., and Vereecken, H.: Sensitivity of simulated soil heterotrophic respiration to temperature and moisture reduction functions, Geoderma, GEODER-09851, doi:10.1016/j.geoderma.2008.01.026, in press, 2008. 1885

5 Borken, W., Davidson, E. A., Savage, K., Gaudinski, J., and Trumbore, S. E.: Drying and wetting effects on carbon dioxide release from organic horizons, Soil Sci. Soc. Am. J., 67, 1888–1896, 2003. 1870

Chen, X. Y., Eamus, D., and Hutley, L. B.: Seasonal patterns of soil carbon dioxide efflux from a wet-dry tropical savanna of northern Australia, Aust. J. Bot., 50, 43–51, 2002. 1870

10 Conen, F., Leifeld, J., Seth, B., and Alewell, C.: Warming mineralises young and old carbon equally, Biogeosciences, 3, 515–519, 2006, http://www.biogeosciences.net/3/515/2006/. 1885

Davidson, E. A. and Janssens, I. A.: Temperature sensitivity of soil carbon decomposition and feedbacks to climate change, Nature, 440, 165–173, 2006. 1869, 1879, 1885

15 Davidson, E. A., Belk, E., and Boone, R. D.: Soil water content and temperature as independent or confounded factors controlling soil respiration in a temperate mixed hardwood forest, Global Change Biol., 4, 217–227, 1998. 1869, 1870, 1879

deForest, J. L., Noormets, A., McNulty, S. G., Sun, G., Tenney, G., and Chen, J.: Phenophases alter the soil respiration-temperature relationship in an oak-dominated forest, Int. J. Biometeorol., 51, 135–144, 2006. 1870, 1881

20 de Vries, D. A.: Thermal properties of soils, in: Physics of Plant Environment, edited by: van Wijk, W. R., North-Holland, Amsterdam, The Netherlands, 210–233, 1963. 1886

Dugas, W. A.: Micrometeorological and Chamber Measurements of CO_2 Flux from Bare Soil, Agr. Forest Meteorol., 67, 115–128, 1993. 1870

25 Fang, C., Moncrieff, J. B., Gholz, H. L., and Clark, K. L.: Soil CO_2 efflux and its spatial variation in a Florida slash pine plantation, Plant Soil, 205, 135–146, 1998. 1870

Fang, C. M., Smith, P., Moncrieff, J. B., and Smith, J. U.: Similar response of labile and resistant soil organic matter pools to changes in temperature, Nature, 433, 57–59, 2005. 1885

Fierer, N., Allen, A. S., Schimel, J. P., and Holden, P.: Controls on microbial CO_2 production: a

30 comparison of surface and subsurface horizons, Global Change Biol., 9, 1322–1332, 2003. 1879

Gaumont-Guay, D., Black, T. A., Griffis, T. J., Barr, A. G., Jassal, R. S., and Nesic, Z.: Inter-

Temperature measurement depth effects

A. Graf et al.

Title Page

Abstract	Introduction
Conclusions	References
Tables	Figures

◀   ▶|

◀   ▶

Back   Close

Full Screen / Esc

Printer-friendly Version

Interactive Discussion

preting the dependence of soil respiration on soil temperature and water content in a boreal aspen stand, Agr. Forest Meteorol., 140, 220–235, 2006. 1869, 1874, 1877, 1881

Graf, A., Kuttler, W., and Werner, J.: Mulching as means to exploit dewfall for arid agriculture?, Atmos. Res., 87, 369–376, 2008. 1886

5 Hanson, P. J., Edwards, N. T., Garten, C. T., and Andrews, J. A.: Separating root and soil microbial contributions to soil respiration: A review of methods and observations, Biogeochemistry 48, 115–146, 2000. 1878

Hashimoto, S. and Komatsu, H.: Relationships between soil CO_2 concentration and CO_2 production, temperature, water content, and gas diffusivity: implications for field studies through
10 sensitivity analyses, J. Forest Res. –JPN, 11, 41–50, 2006. 1869

Herbst, M., Hellebrand, H. J., Bauer, J., Huisman, J. A., Simunek, J., Weihermüller, L., Graf, A., Vanderborght, J., and Vereecken, H.: Multiyear heterotrophic soil respiration: evaluation of a coupled CO_2 transport and carbon turnover model, Ecol. Model., doi:10.1016/j.ecolmodel.2008.02.007, in press, 2008. 1883

15 Heusinkveld, B. G., Jacobs, A. F. G., Holtslag, A. A. M., and Berkowicz, S. M.: Surface energy balance closure in an arid region. Role of soil heat flux, Agr. Forest Meteorol., 122, 21–37, 2004. 1886

Hirano, T., Kim, H., and Tanaka, Y.: Long-term half-hourly measurement of soil CO_2 concentration and soil respiration in a temperate deciduous forest, J. Geophys. Res. Atmos., 108(D20),
20 4631, doi:10.1029/2003JD003766, 2003. 1869, 1887

Humphreys, E. R., Black, T. A., Morgenstern, K., Cai, T. B., Drewitt, G. B., Nesi, Z., and Trofymow, J. A.: Carbon dioxide fluxes in coastal Douglas-fir stands at different stages of development after clearcut harvesting, Agr. Forest Meteorol., 140, 6–22, 2006. 1870

Kätterer, T., Reichstein, M., Andrén, O., and Lomander, A.: Temperature dependence of organic
25 matter decomposition: a critical review using literature data analyzed with different models, Biol. Fert. Soils, 27, 258–262, 1998. 1884

Khomik, M., Arain, M. A., and McCaughey, J. H.: Temporal and spatial variability of soil respiration in a boreal mixedwood forest, Agr. Forest Meteorol., 140, 244–256, 2006. 1869, 1874, 1877, 1881

30 Kim, J. and Verma, S. B.: Soil CO_2 flux in a Minnesota peatland, Biogeochemistry, 18, 37–51, 1992. 1870

Kirschbaum, M. U. F.: The temperature dependence of organic-matter decomposition – still a topic of debate, Soil Biol. Biochem., 38, 2510–2518, 2006. 1885

Temperature measurement depth effects

A. Graf et al.

Knorr, W., Prentice, I. C., House, J. I., and Holland, E. A.: Long-term sensitivity of soil carbon turnover to warming, Nature, 433, 298–301, 2005. 1879, 1885

Larinova, A. A., Yevdokimov, I. V., and Bykhovets, S. S.: Temperature response of soil respiration is dependent on concentration of readily decomposable C, Biogeosciences, 4, 1073–1081, 2007,
http://www.biogeosciences.net/4/1073/2007/. 1885

Law, B. E., Falge, E., Gu, L., et al.: Environmental controls over carbon dioxide and water vapor exchange of terrestrial vegetation, Agr. Forest Meteorol., 113, 97–120, 2002. 1870

Lloyd, J. and Taylor, J. A. On the temperature-dependence of soil respiration, Funct. Ecol., 8, 315–323, 1994. 1869, 1884

Lou, Y. S., Li, Z. P., and Zhang, T. L.: Soil CO_2 flux in relation to dissolved organic carbon, soil temperature and moisture in a subtropical arable soil of China, J. Environ. Sci.-China, 15, 715–720, 2003. 1870

Moyano, F. E., Kutsch, W. L., and Rebmann, C.: Soil respiration fluxes in relation to photosynthetic activity in broad-leaf and needle-leaf forest stands, Agr. Forest Meteorol., 148, 135–143, 2008. 1870, 1878

Novak, M. D.: Determination of soil carbon dioxide source-density profiles by inversion from soil-profile gas concentrations and surface flux density for diffusion-dominated transport, Agr. Forest Meteorol., 146, 189–204, 2007. 1883

Novick, K. A., Stoy, P. C., Katul, G. G., Ellsworth, D. S., Siqueira, M. B. S., Juang, J., and Oren, R.: Carbon dioxide and water vapor exchange in a warm temperate grassland, Oecologia, 138, 259–274, 2004. 1870

Perrin, D., Laitat, E., Yernaux, M., and Aubinet, M.: Modelling the response of forest soil respiration fluxes to the main climatic variables, Biotechnol. Agron. Soc. Environ., 8, 15–25, 2004. 1869, 1874, 1877, 1880

Raich, J. W. and Schlesinger, W. H.: The global carbon dioxide flux in soil respiration and its relationship to vegetation and climate, Tellus, 44(B), 81–99, 1992.

Reichstein, M., Kätterer, T., Andrèn, O., Ciais, P., Schulze, E. D., Cramer, W., Papale, D., and Valentini, R.: Temperature sensitivity of decomposition in relation to soil organic matter pools: critique and outlook, Biogeosciences, 2, 317–321, 2005,
http://www.biogeosciences.net/2/317/2005/. 1885

Sanderman, J., Amundson, R. G., and Baldocchi, D. D.: Application of eddy covariance measurements to the temperature dependence of soil organic matter mean residence time,

Global Biogeochem. Cy., 17, 1061, doi:10.1029/2001GB001833, 2003. 1872

Savage, K. E. and Davidson, E. A.: A comparison of manual and automated systems for soil CO_2 flux measurements: trade-offs between spatial and temporal resolution, J. Exp. Bot., 54, 891–899, 2003. 1870

5 Shi, P. L., Zhang, X. Z., Zhong, Z. M., and Ouyang, H.: Diurnal and seasonal variability of soil CO_2 efflux in a cropland ecosystem on the Tibetan Plateau, Agr. Forest Meteorol., 137, 220–233, 2006. 1869, 1874, 1877, 1880, 1885

Simunek, J. and Suarez, D. L.: Modeling of carbon-dioxide transport and production in soil. 1. Model development, Water Resour. Res., 29, 487–497, 1993. 1887

10 Solomon, S., Qin, D., Manning, M., et al. (Eds.): Climate Change 2007: The Physical Science Basis, Contribution of Working Group I to the Fourth Assessment Report of the Intergovernmental Panel on Climate Change Cambridge University Press, Cambridge, United Kingdom and New York, NY, USA, 501–539, 2007. 1883

Takahashi, A., Hiyama, T., Takahashi, H. A., and Fukushima, Y.: Analytical estimation of the
15 vertical distribution of CO_2 production within soil: application to a Japanese temperate forest, Agr. Forest Meteorol., 126, 223–235, 2004. 1870

Takle, E. S., Massmann, W. J., Brandle, J. R., et al.: Influence of high-frequency ambient pressure pumping on carbon dioxide efflux from soil, Agr. Forest Meteorol., 124, 193–206, 2004. 1887

20 Tang, J. W., Baldocchi, D. D., Qi, Y., and Xu, L. K.: Assessing soil CO_2 efflux using continuous measurements of CO_2 profiles in soils with small solid-state sensors, Agr. Forest Meteorol., 118, 207–220, 2003. 1869, 1879, 1880, 1887

Tang, J. W., Baldocchi, D., and Xu, L. K.: Tree photosynthesis modulates soil respiration on a diurnal time scale, Global Change Biol., 11, 1298–1304, 2005. 1878

25 Tang, J., Bolstad, P. V., Desai, A. R., Martin, J. G., Cook, B. D., Davis, K. J., and Carey, E. V.: Ecosystem respiration and its components in an old-growth forest in the Great lakes region of the United States, Agr. Forest Meteorol., 148, 171–185, 2008. 1870

Verhoef, A., van den Hurk, B. J. J. M., Jacobs, A. F. G., and Heusinkveld, B. G.: Thermal soil properties for vineyard (EFEDA-I) and savanna (HAPEX-Sahel) sites, Agr. Forest Meteorol.,
30 78, 1–18, 1996. 1874, 1886

Wang, C., Yang, J., and Zhang, Q.: Soil respiration in six temperate forests in China, Global Change Biol., 12, 2103–2114, 2006. 1869, 1877

Weber, S., Graf, A., and Heusinkveld, B. G.: Accuracy of soil heat flux plate measurements in

Temperature measurement depth effects

A. Graf et al.

coarse substrates –Field measurements versus a laboratory test, Theor. Appl. Climatol., 89, 109–114, 2007. 1885

Weihermüller, L., Huisman, J. A., Graf, A., Herbst, M., and Vereecken, H.: Multistep outflow experiments for the simultaneous determination of soil physical and CO_2 production parameters, EGU General Assembly, Vienna, Austria, 16–20 April 2007, EGU07-A-01742, 2007a. 1883

Weihermüller, L., Huisman, J. A., Lambot, S., Herbst, M., and Vereecken, H.: Mapping the spatial variation of soil water content at the field scale with different ground penetrating radar techniques, J. Hydrol., 340, 205–216, 2007b. 1872

Werner, D., Grathwohl, P., and Höhener, P.: Review of field methods for the determination of the tortuosity and effective gas-phase diffusivity in the vadose zone, Vadose Zone J., 3, 1240–1248, 2004. 1879, 1881, 1887

Xu, M. and Qi, Y.: Spatial and seasonal variations of Q_{10} determined by soil respiration measurements at a Sierra Nevada forest, Global Biogeochem. Cy., 15, 687–696, 2001. 1869, 1881

Yuste, J. C., Janssens, I. A., Carrara, A., and Ceulemans, R.: Interactive effects of temperature and precipitation on soil respiration in a temperate maritime forest, Tree Physiol., 23, 1263–1270, 2003. 1870

Yuste, J. C., Janssens, I. A., Carrara, A., and Ceulemans, R.: Annual Q(10) of soil respiration reflects plant phenological patterns as well as temperature sensitivity, Global Change Biol., 10, 161–169, 2004. 1881, 1884

Zmarsly, E., Kuttler, W., and Pethe, H.: Meteorologisch-klimatologisches Grundwissen, Ulmer, Stuttgart, Germany, 2002. 1881, 1886

Temperature measurement depth effects

A. Graf et al.

Temperature measurement depth effects

A. Graf et al.

Table 1. Studies providing multiple Q_{10} values due to multiple temperature measurement depths.

	reference	method	site	frequency	period
1	Xu and Qi (2001)	chamber	ponderosa pine plantation, Sierra Nevada, USA[a]	≥ 1 month^{-1}, ≥ 6 day^{-1}	Jun 1998–Aug 1999
2	Hirano et al. (2003)	profile	temperate deciduous forest, Japan	2 h^{-1}	May 2000–Nov 2000
3	Tang et al. (2003)	profile	oak-grass savannah, Sierra Nevada, USA	2 h^{-1}	Jul 2002–Nov 2002
4	Perrin et al. (2004)	chamber	beech forest, Ardennes, Belgium	2 h^{-1}	Jun 2000–Jul 2003
5	Gaumont-Guay et al. (2006)	chamber	boreal aspen forest, central Canada	2 h^{-1}	Jan 2001–Feb 2001
6	Khomik et al. (2006)	chamber	boreal forest, eastern Canada	1 month^{-1} [b], not in winter	Jul 2003–Jul 2005
7	Shi et al. (2006)	chamber	irrigated farmland, Tibetan Plateau	≥ 1 month^{-1}, ≥ 2 day^{-1} [c]	Sep 1999–Aug 2001
8	Wang et al. (2006)	chamber	six different forests, north-eastern China	2 week^{-1}	Apr 2004–Oct 2005

[a] results given separately for two sites
[b] moring and afternoon of the measurement day in summer, once per day in transition months
[c] on two days per month in summer, 8 times at some days

Table 2. Results of model validation under different settings.

source profile	domain depth	optimal input Q_{10}	RMSE
1 (>-30 cm), 0 (<-30 cm)	50 cm	5.9	0.16
1 (>-30 cm), 0 (<-30 cm)	120 cm	5.3	0.80
measured C_{org}	50 cm	6.2	0.21
measured C_{org}	120 cm	5.9	1.20

Temperature measurement depth effects

A. Graf et al.

Temperature climate characterization

i	period length τ_i	phase shift Δt_i	Amplitude A_i at z_{ref}
1	1 yr	260 d	variant input
2	1 d	15 h	variant input
3	0.5 d	1 h	variant input
4...	other		not used in this study

Depth of known amplitudes: z_{ref}

Study schedule
Start: variant input
Time step: here, 1h
length: variant input

Annual Average Temperature
T_{avg}: variant input

Soil properties

depth z	thermal diffusivity D_T	temperature sensitivity Q_{10} or E_a	source strength SR_{Tref}	eff. CO_2 diffusivity D_{CO2}/θ
0				
1 cm				
2 cm		variant input		
...				
50 cm				

Eq. B3 (stepwise)

Eq. B3

Eq. A1 or A2

Phase shifts Δt_i, Amplitudes A_i

z	$i=1$	$i=2$	...
0			
1 cm			
2 cm		$[\cdot\cdot]$	
...			
50 cm			

Temperature $T(z,t)$

z	t_1	t_2	...
0			
1 cm			
2 cm		$[\cdot\cdot]$	
...			
50 cm			

Respiration $SR(T)$

z	t_1	t_2	...
0			
1 cm			
2 cm		$[\cdot\cdot]$	
...			
50 cm			

$\sum_z SR$

F — CO_2 diffusion? — T

Eq.C2 (sub-timesteps)

(Eq. A1 or A2)$^{-1}$

Resulting profile

z	Q_{10}	R^2
0		
1 cm		
2 cm	output	
...		
50 cm		

Efflux(t)

t_1	t_2	...
	[...]	

Concentration $c(z,t)$

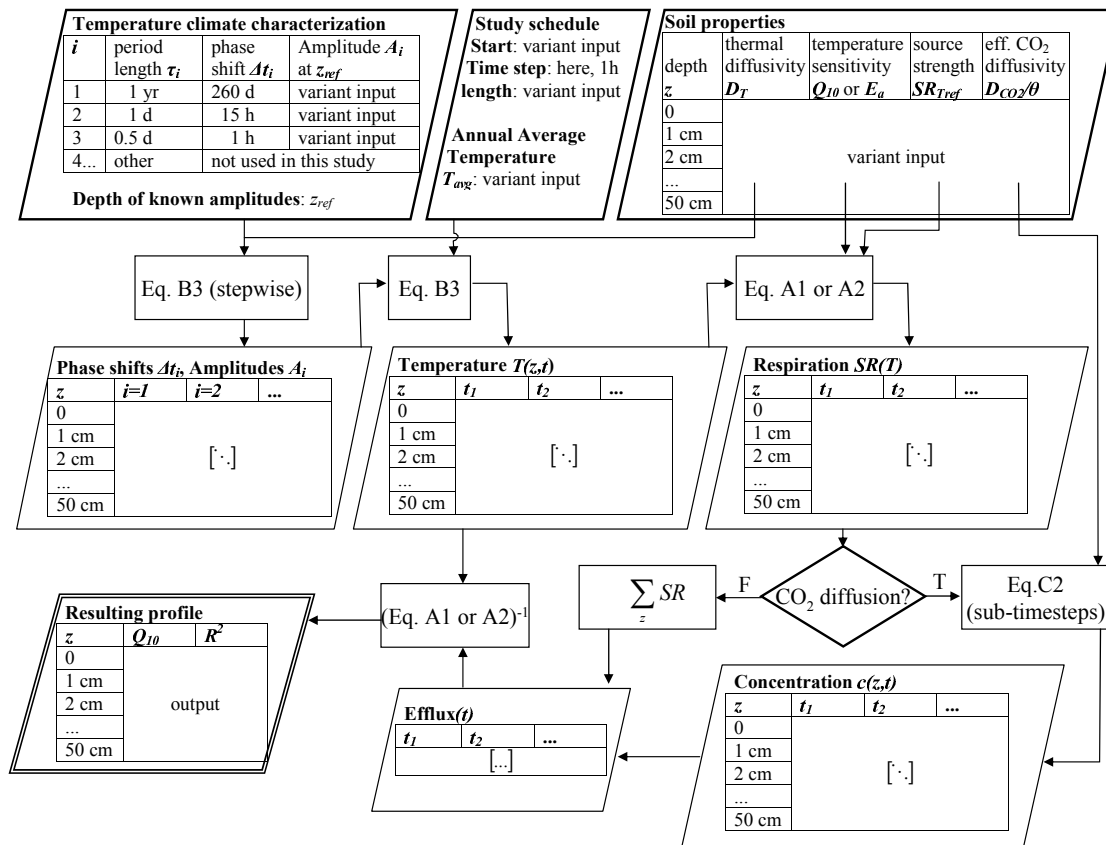| z	t_1	t_2	...
0			
1 cm			
2 cm		$[\cdot\cdot]$	
...			
50 cm			

Fig. 1. Overview of the model architecture. Bold outline: Input parameters; doubled outline: Final output. Symbols are explained in the Appendix.
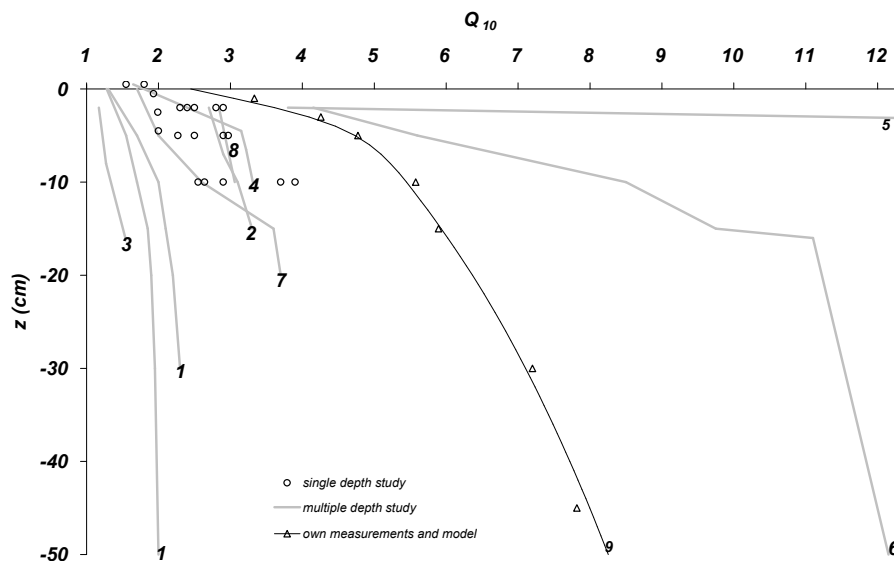
Fig. 2. Empirical apparent Q_{10} as a function of temperature measurement depth z. Numbers refer to the study bibliography given in Table 2, single depth references are listed in the methods section. Depths >0 denote air temperature (height not to scale).
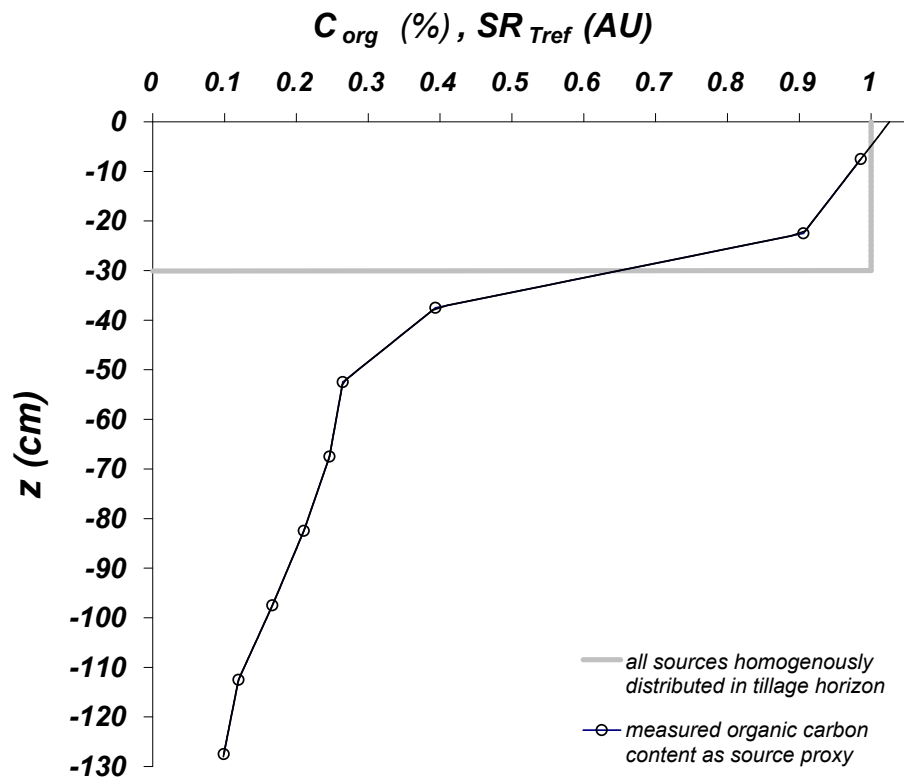
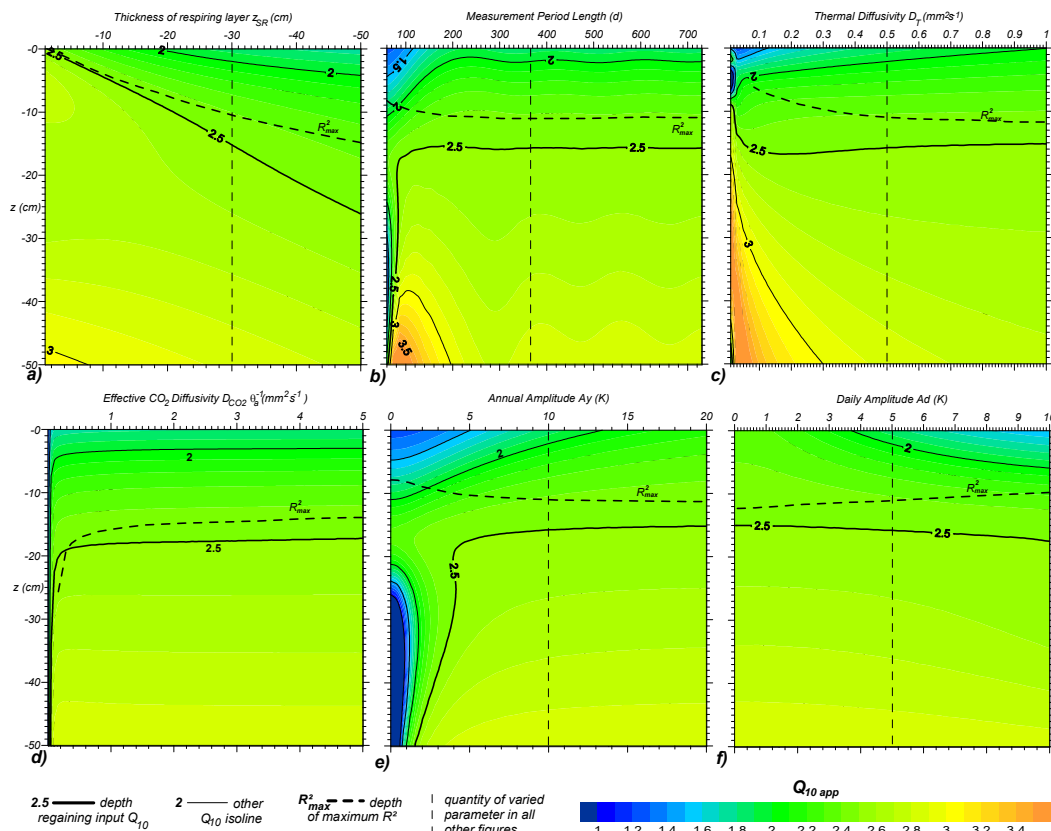**Fig. 3.** Source strength profiles used in the model validation.

Fig. 4. Apparent Q_{10} resulting from simulated hourly flux measurements as a function of temperature measurement depth z and: **(a)** thickness of a homogenous respiring layer, **(b)** measurement period, **(c)** thermal diffusivity (one for all depths), **(d)** effective CO_2 diffusivity, **(e)** annual temperature amplitude, **(f)** diurnal temperature amplitude. D_{CO_2} is infinite in all but (d).